

# INSTALLATION AND PERFORMANCE OF THE STABLE INSTRUMENTATION AT HALLEY

J. C. KING and P. S. ANDERSON

*British Antarctic Survey, Natural Environment Research Council, High Cross,  
Madingley Road, Cambridge CB3 0ET, UK*

**ABSTRACT.** The instrumentation installed at Halley for STABLE (the STable Antarctic Boundary Layer Experiment) is described. Turbulence measurements were made using three ultrasonic anemometers, with conventional cup anemometers providing additional profile measurements. Temperature profiles were measured by platinum resistance thermometers and a Sodar system was used to provide a continuous record of boundary layer structure. Instruments generally performed well although blowing snow and rime ice accumulation affected their performance at times.

## INTRODUCTION

In 1986 the British Antarctic Survey undertook a major programme of atmospheric boundary-layer measurements at Halley (75.6° S, 26.7° W). Attention was concentrated on the stably-stratified boundary layer and the project was known as STABLE (the STable Antarctic Boundary Layer Experiment). Measurements started in February and continued through the winter until the instrumentation was dismantled in November. Halley was chosen for these investigations since it is situated on a broad flat ice shelf (the Brunt Ice Shelf) which offers a homogeneous and unobstructed fetch from most wind directions. Strong surface inversions are common and, during the three months of winter darkness, steady-state conditions can exist for prolonged periods. Previous studies of the stable boundary layer in mid-latitudes (e.g. Webb, 1970; Businger and others, 1971; Caughey and others, 1979) have had to contend with the complications of inhomogeneous terrain and diurnal variation and it was hoped that this study would reveal some of the basic physics of the stable boundary layer. Instrumentation for use during the Antarctic winter must be robust and reliable. It is only recently that ultrasonic anemometers have become available and opened up the possibility of making long-term direct measurements of turbulent fluxes under such conditions.

The experiment had two related goals; firstly a detailed study of the structure of turbulence in the stably-stratified surface layer and secondly an investigation of the wave-like disturbances which had been observed in the lower troposphere at Halley (Darby and Mobbs, 1987). In order to fulfil the first objective, instrumentation for measuring both turbulence and mean profiles of wind and temperature was installed on a 30-m mast and further instruments to examine the components of the energy balance of the snow surface were installed close by. The second objective required measurements over a greater depth of the lower atmosphere; these were obtained from a Sodar system and by radiosondes. Additionally, some instruments were installed away from the 30-m mast to produce an array which could be used to study the horizontal propagation of waves in the lower troposphere.

Scientific results from the experiment are presented elsewhere (King and others, 1987; Rees and Mobbs, 1987). In this paper we describe the instruments used and their deployment on site and our data logging system. Detailed reports on the performance of each instrument are also given.

## DEPLOYMENT OF THE INSTRUMENTS

*Site characteristics*

Halley station is situated towards the seaward edge of the Brunt Ice Shelf. The shelf extends inland of the station for approximately 40 km with no significant slope or other topography (Thomas, 1973). Beyond this, there is a steep rise up to the continental plateau. The snow surface at Halley is characterized by small sastrugi which have a height of a few centimetres and continually alter in form with changing weather conditions (Tribble, 1964). Undulations with an amplitude of 5 m and wavelengths of about 1 km exist over parts of the shelf (Thomas, 1973). Measurements on a similar Antarctic ice shelf site (König, 1985) have shown that the aerodynamic roughness length of such surfaces is small – about  $10^{-4}$  m – and is related to the fine structure of the snow surface rather than features such as sastrugi.

Table I. Deployment of instruments on the 30-m mast. Heights of instruments are as of 28 January 1986

<i>Instrument</i>	<i>Height above surface at installation (m)</i>	<i>Instrument</i>	<i>Height above surface at installation (m)</i>
Ultrasonic anemometer	32.9	Platinum-resistance thermometer	8.7
Platinum-resistance thermometer	31.4	Ultrasonic anemometer	5.6
Cup-anemometer	24.4	Platinum-resistance thermometer	4.8
Ultrasonic anemometer	17.4	Platinum-resistance thermometer	2.8
Platinum-resistance thermometer	16.8	Cup-anemometer	2.6
Cup-anemometer and wind vane	8.7		

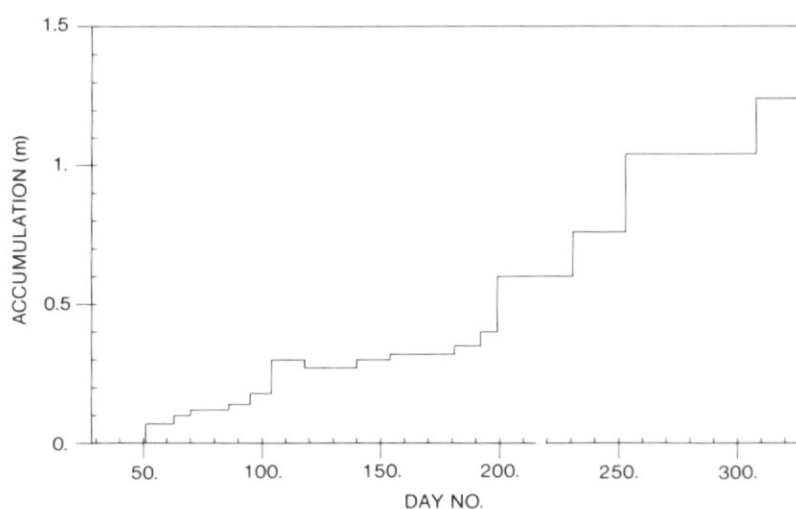


Fig. 1. Snow accumulation at the base of the 30-m mast during STABLE. Day 1 = 1 January 1986.

Near-surface winds blow most frequently from the sector  $090 \pm 20^\circ$ , with a secondary maximum between  $200$  and  $270^\circ$ . Wind speeds are generally moderate with an annual mean of about  $6.5 \text{ m s}^{-1}$ . Winter surface temperatures are typically around  $-30^\circ\text{C}$  but may fall as low as  $-55^\circ\text{C}$  under calm conditions.

There is a net accumulation of snow at the site throughout the year. The accumulation rate varies from about  $0.9 \text{ m year}^{-1}$  over the open ice shelf (Limbert, 1963) to over twice this rate in the vicinity of the base buildings. The effect of this accumulation was progressively to reduce the effective heights of all of the instruments during the year. Heights at which the instruments were initially deployed are given in Table I, and Fig. 1 shows snow accumulation at the base of the 30-m mast as a function of time, from which the effective height of any instrument at a given time can be deduced.

The absolute humidity of the air is generally small, due to the low temperatures. However, freezing fog occurred quite frequently during the 1986 winter, leading to large accumulations of rime ice on the instruments. These conditions could persist for several days. The winter of 1986 seems to have been somewhat exceptional in this respect; during previous winters icing of instruments was a problem on relatively few days.

#### *Overview of the instrumentation*

Fig. 2 shows the general layout of the measurement site which is approximately 300 m south-east of the main base buildings. The 30-m mast was sited to give optimum exposure to winds from the prevailing direction ( $090^\circ$ ) and unobstructed exposure from a wide range of directions. The mast was manufactured by South Midlands Communications (Unimast 40 series) and was of triangular, open lattice construction with a side length of 400 mm. It was erected on a base section which had been installed on a buried wooden foundation early in 1985 to ensure a firm footing, and was thus somewhat over 30 m high on installation. The instruments mounted on this mast and the heights at which they were installed are listed in Table I.

Turbulence measurements were made using three 3-component ultrasonic anemometer/thermometers (Kaijo Denki model DAT-100). Each system comprised a sensing head (type TR-61A) and junction box (mounted on the mast) and an electronic analyzer unit (situated in the logging hut) which produced analogue outputs corresponding to the three orthogonal wind components and to temperature. The highest of these instruments was mounted on top of a 1.5-m extension to the top of the mast, made of 50 mm diameter tubing. The lower two instruments were mounted on the end of booms which extended 1.2 m beyond the mast in a direction of  $120^\circ$ . This ensured that the instrument was measuring flow undisturbed by the mast for wind directions from  $040$  to  $200^\circ$ . Further details on the installation of the ultrasonic anemometers are given in the section on instrument performance.

Three cup-anemometers (Vector Instruments A100) were mounted on booms at intermediate levels to provide additional measurements of the wind profile. They were equipped with 6 W heater elements to combat icing problems. Additionally, a potentiometer wind vane (Vector Instruments W200P) was installed at one level.

Temperature profiles were measured using platinum resistance thermometers in fan-ventilated radiation shields (Vector Instruments T302) at five levels. These were arranged as a bridge circuit (see section on instrument performance) to produce temperature differences over four height intervals. Absolute temperature was obtained from the lowest ultrasonic anemometer/thermometer.

The surface energy balance instrumentation consisted of a Kew-pattern radiation

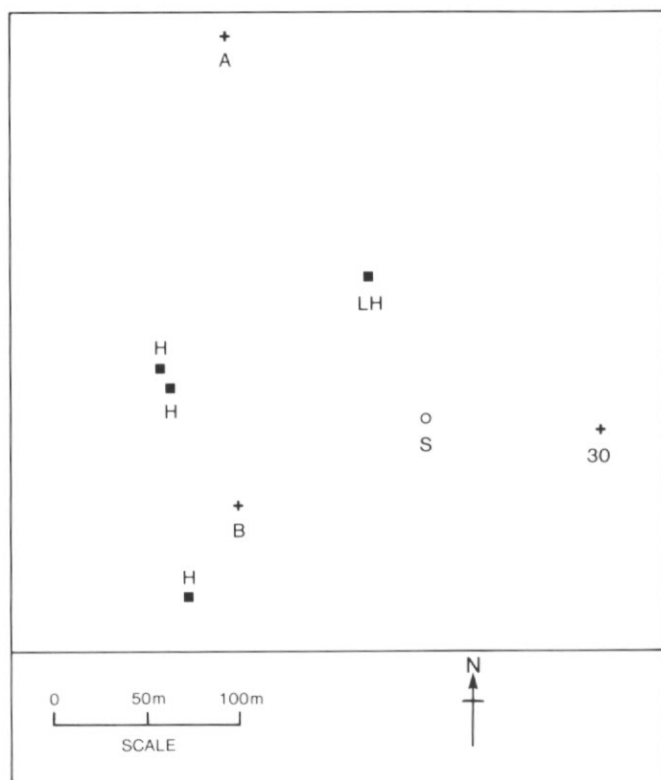


Fig. 2. A sketch plan of the experimental site. 30, 30-m mast. A, B, 'remote' masts carrying instruments at 8 m. S, Sodar. LH, Logging Hut. H, other huts.

balance meter and a system for measuring sub-snow temperature profiles (see section on instrument performance). These were installed a short distance from the logging hut on an area of snow which was kept as free from disturbance as possible throughout the experiment.

The Sodar was manufactured by Sensitron. A platform for the acoustic antenna was constructed about 100 m from the logging hut. Sodar returns were displayed on a facsimile recorder housed in the hut.

Two 'remote' masts (positions marked on Fig. 2) completed the horizontal array. These each carried a cup anemometer and wind vane, identical to those used on the main mast, at about 8 m above surface level. It was not possible to distribute heater power to these masts and icing could render these instruments inoperative for prolonged periods.

This concludes the description of the instruments installed specifically for STABLE. Use was also made of the radiosonde facility already installed at Halley – a Vaisala micro-CORA system which uses the OMEGA navigational aid for windfinding. The three-hourly synoptic surface observations made at Halley also proved useful in interpreting and checking our results.

## DATA LOGGING

Analogue signals from instruments on the 30-m mast, the 'remote' masts and the surface energy balance system were led by cable to the logging hut. Signal cables entered a junction box through feed-through capacitative filters to remove any radio frequency interference before distribution to the appropriate signal conditioning circuits. These circuits were all designed to produce analogue signals in the range  $\pm 5$  V for compatibility with the data logging system. All signals were low-pass filtered before logging.

The data logger comprised two independent microcomputer systems (based on the 6809 microprocessor) which could communicate via a parallel interface. One system, 'machine 1', controlled four 12-bit analogue-to-digital convertors, each of which was multiplexed to eight analogue inputs giving a total of 32 available input channels. Machine 1 ran a fixed programme which would sample the analogue channels at selected intervals and organize the samples in a buffer. The other system, 'machine 2', ran user programmes under the FLEX operating system. Machine 2 was able to send commands to machine 1 to select sampling rates, commence or stop continuous sampling and request transmission of a block of samples. The user programme in machine 2 was able to process the incoming samples and store the results on either floppy disc or industry-standard 9-track digital magnetic tape.

Two data logging programmes were used. For continuous operation, the processing power of machine 2 was used to compute means of all sampled channels over 10-minute analysis periods. Additionally, the variances  $\overline{u'u'}$ ,  $\overline{v'v'}$ ,  $\overline{w'w'}$ ,  $\overline{T'T'}$  and cross variances  $\overline{u'w'}$ ,  $\overline{v'w'}$ ,  $\overline{u'v'}$ ,  $\overline{u'T'}$ ,  $\overline{v'T'}$ ,  $\overline{w'T'}$  were computed for each ultrasonic anemometer ( $u$ ,  $v$ ,  $w$  and  $T$  are the three components of velocity and temperature respectively. Primes denote fluctuations and overbars 10-minute means). These 10-minute means were recorded on floppy disc (later archived to magnetic tape) and form our basic turbulence data set. The 10-minute averaging period is a compromise between obtaining stable turbulence statistics and excluding the effects of large-scale motions or trends. The sampling rate for the ultrasonic anemometers had to be limited to 5 Hz to enable machine 2 to carry out this synchronous processing; however this rate should be sufficient for the calculation of turbulence statistics. Other instruments were sampled at 1 Hz. Over 2000 hours of 10-minute means were collected between March and September inclusive.

During selected periods, the 'raw' data passed to machine 2 could be recorded directly on magnetic tape without any processing being carried out. In this mode of logging, the ultrasonic anemometers could be sampled at 20 Hz, which is the frequency limit imposed by the internal electronics of the anemometer and is consistent with the spatial averaging implied by the 200 mm ultrasonic path length. The other instruments had much longer characteristic time constants and were again sampled at 1 Hz. As a slight variant on this programme, the data could be block averaged to form 1-s or 10-s samples before being recorded on tape. These raw data tapes were used for studies of the spectral characteristics of turbulence and waves.

Each week, known voltages were injected into all 32 data-logger channels to check for any changes in multiplexer or analogue-to-digital converter characteristics. No significant changes occurred during the experiment.

## INSTRUMENT PERFORMANCE

*Ultrasonic anemometers*

The Kaijo Denki ultrasonic anemometers were manufactured to the same specification as those supplied to the Japanese Antarctic Research Expedition (Adachi, 1974; Kobayashi and Ishida, 1979) and operated well at the low temperatures experienced. Great care was taken to avoid damaging or straining the anemometer heads during installation on the 30-m mast since slight changes in head geometry will change the calibration of the instrument. The heads were levelled as accurately as possible using the spirit level incorporated into the instrument and the azimuth of the head was measured using a hand-held compass. Levelling errors were estimated to be no more than  $\pm 2^\circ$  and the azimuth measurement has a similar uncertainty.

It is possible to check the levelling of the heads by examining the behaviour of the ratio of apparent mean vertical velocity to horizontal velocity,  $\bar{w}/\bar{u}$ , as a function of wind direction relative to the head. Close to the ground, we expect the true mean vertical velocity to be zero, hence a simple tilt of the instrument would make  $\bar{w}/\bar{u}$  appear to be a sinusoidal function of wind direction. However, any distortion of the flow by the head itself or by its mounting may induce a mean vertical velocity. Our measurements for the lower two instruments (which were mounted on horizontal booms) suggest that the heads were tilted by about  $2^\circ$  and that flow distortion by the mounts caused a flow tilt of about  $0.9^\circ$ , which showed little dependence on wind direction. The upper instrument was mounted directly above the top of the mast and could be levelled more accurately. Measurements of  $\bar{w}/\bar{u}$  for this instrument show little variation with wind direction and would suggest that the instrument was truly level but that flow distortion by the mount was again about  $0.9^\circ$ . We have allowed for instrument tilt in our analysis of the ultrasonic anemometer data by rotating all quantities into a level coordinate frame but we have not attempted to correct the results for distortion of the flow by the instrument mount.

Ice build-up on the ultrasonic anemometer heads proved to be a problem during some periods with low wind speeds. Feathery rime would build up preferentially on the transducer which was pointing most nearly into the wind. Eventually this would cause the anemometer to fail to detect the occasional pulse, giving rise to 'spikes' of full scale output. A similar effect occurred during high wind speeds which were accompanied by falling or blowing snow. Impacting of snow particles on the transducers would again produce spurious readings. Fig. 3 shows the observed standard deviation of horizontal wind speed,  $\sigma_u$ , as a function of mean wind speed,  $\bar{u}$ . There are two clear groups of outlying points with an anomalously high standard deviation: those at low wind speeds where icing was a problem and a second group with  $u > 12 \text{ m s}^{-1}$  where falling or blowing snow was causing the spurious readings. It has proved possible to use the criterion:

$$\sigma_u/\bar{u} > 0.122$$

to identify data points affected by icing.

Two temperature outputs are available from each ultrasonic anemometer: a coarse resolution measurement of absolute temperature (range  $\pm 50^\circ\text{C}$ ) and a fine resolution measurement with a range of  $\pm 5^\circ\text{C}$  about a pre-set central value. The temperature measurement is produced by measuring the speed of sound,  $c$ , along the vertical path. This is related to temperature through the equation:

$$c^2 = AT(1 + 0.51q),$$

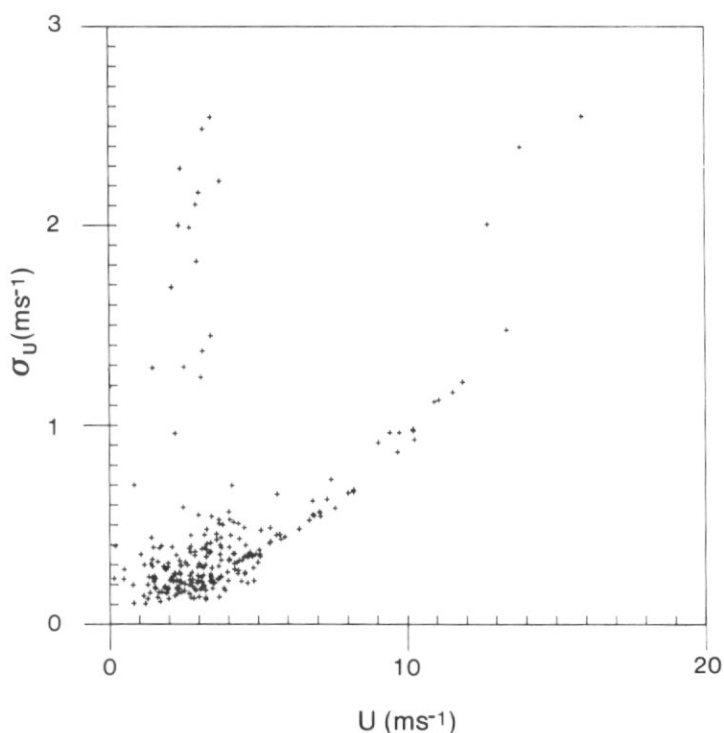


Fig. 3. Standard deviation of wind speed as a function of mean wind speed for data collected from the lowest ultrasonic anemometer during June 1986.

where  $A$  is a constant ( $403 \text{ m}^2 \text{ s}^{-2} \text{ K}^{-1}$  for air),  $T$  is the absolute temperature and  $q$  the specific humidity. Thus the ultrasonic anemometer/thermometer actually measures virtual temperature, but at the low temperatures prevailing at Halley,  $q$  is so small as to make the difference negligible. However, the measurement of  $c$  itself is contaminated by the component of wind blowing across the path used for the measurement (Kaimal, 1969) and the use of temperatures so derived in determining heat fluxes,  $\overline{w'T'}$ , has been questioned. The error in the heat flux,  $\overline{w'T'}$ , is approximately

$$E = \frac{2T\bar{u}}{c^2} \overline{u'w'}$$

We have examined values of the heat flux error term and found it to be typically less than 5% of  $\overline{w'T'}$ , which has given us some confidence in these measurements. Although an independent measurement would have been desirable, it is unlikely that any other fast-response temperature sensor would have been robust enough to operate through the Antarctic winter. The central temperature was reset manually at least once each day, but during periods of rapid temperature change the fine-resolution temperature could reach full scale. These occasions are easily determined from inspection of the 10-minute average data and can be excluded from the data analysis.

Before installation, all three ultrasonic anemometers were adjusted in accordance with the manufacturer's instructions to give zero output when the heads were placed

in a windless enclosure. This check was carried out again after the anemometers had been deployed for six months and no further adjustment was found necessary, indicating a high stability of calibration.

### *Cup-anemometers*

Individual calibrations for the Vector Instruments cup-anemometers were supplied by the manufacturer. The anemometers and vane on the 30-m mast had heaters fitted to their spindle housings. These ensured that the bearings were kept free of ice under all but the heaviest riming conditions. However, the heating was not sufficient to prevent the build-up of ice on the cups, leading to an uncertainty in the calibration of the anemometer. The instruments on the remote masts were unheated and would seize up during icing conditions. Instruments on the 30-m mast were cleared of ice manually from time to time and all ice would be removed by strong winds.

Following the main experiment, all three cup-anemometers on the 30-m mast were deployed at the same level as the lowest ultrasonic anemometer for a period of intercomparison, the results of which are shown in Fig. 4. Only data points for which the ultrasonic anemometer was not affected by icing have been included. For mean wind speeds greater than about  $5 \text{ m s}^{-1}$ , the cup-anemometer reads about 5% above the 'true' speed as measured by the ultrasonic anemometer. This is in accordance with previous findings that cup-anemometers tend to overspeed in a turbulent flow.

When the windspeed is low, agreement between the cup and ultrasonic

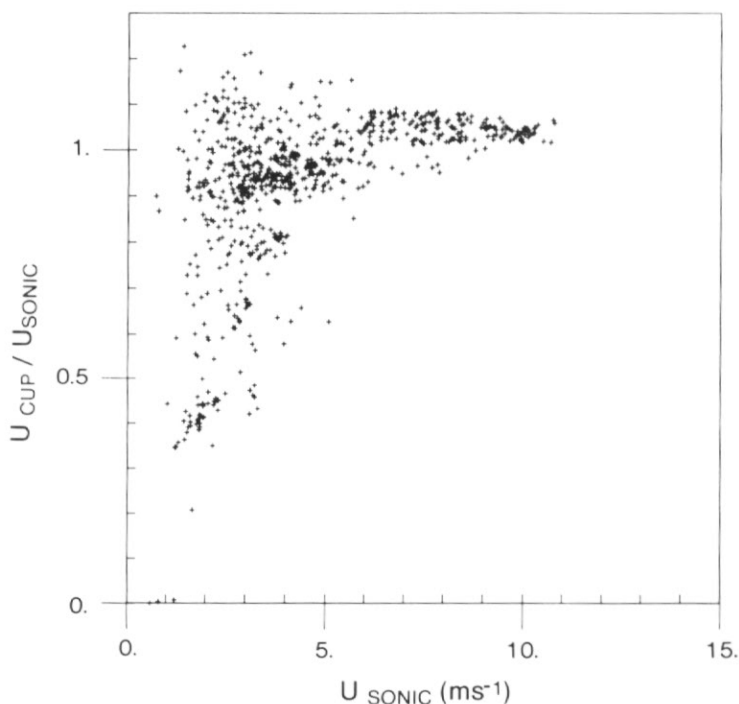


Fig. 4. Variation of the ratio of cup-anemometer to ultrasonic anemometer wind speed with wind speed during the intercomparison experiment.



anemometers is poor, with the cup-anemometer readings generally falling below the 'true' wind speed but showing considerable scatter. It seems likely that this scatter is due to variations in ice build-up – the greater the accumulation of ice, the greater the reduction in the rate of rotation of the cup anemometer for a given wind speed. Since the precise amount of icing at a given time is unknown, it is impossible to adjust the anemometer calibration to allow for icing. Because of these problems, we have only made use of the cup-anemometer wind profiles under strong wind conditions when all ice was removed from the cups and we could be certain of the instrument calibrations.

#### *Ventilated platinum resistance thermometers*

Five aspirated platinum resistance thermometer (PRT) temperature sensors (Vector Instruments type T302), as designed by the Boundary Layer Branch of the Meteorological Office, were used to measure temperature differences over four successive intervals on the 30-m mast. The units consisted of standard  $100\ \Omega$  PRTs (1/3 IN 43760, class B) housed in a triple-walled enclosure and aspirated at  $4\ \text{m s}^{-1}$  by a 12 V AC fan. The design incorporated additional radiation shielding in the form of an umbrella over the top of the housing, to reduce radiation errors for solar elevations in excess of  $66^\circ$ , although the sun never attains this elevation at Halley. The sensors were connected to a difference bridge inside the logging hut using the 4-wire compensation loop method (see Fig. 5). Mounting was by light-alloy U-tube booms attached to the top of the sensors. These proved to be insufficiently rigid in wind speeds in excess of  $20\ \text{m s}^{-1}$ .

The sensitivity of these temperature-sensor shields to solar radiation has been determined as less than  $5 \times 10^{-5}\ \text{K (W m}^{-2}\text{)}^{-1}$  (B. A. Callander, pers. comm.). However, with a high albedo surface, such as is found at Halley, incident radiation

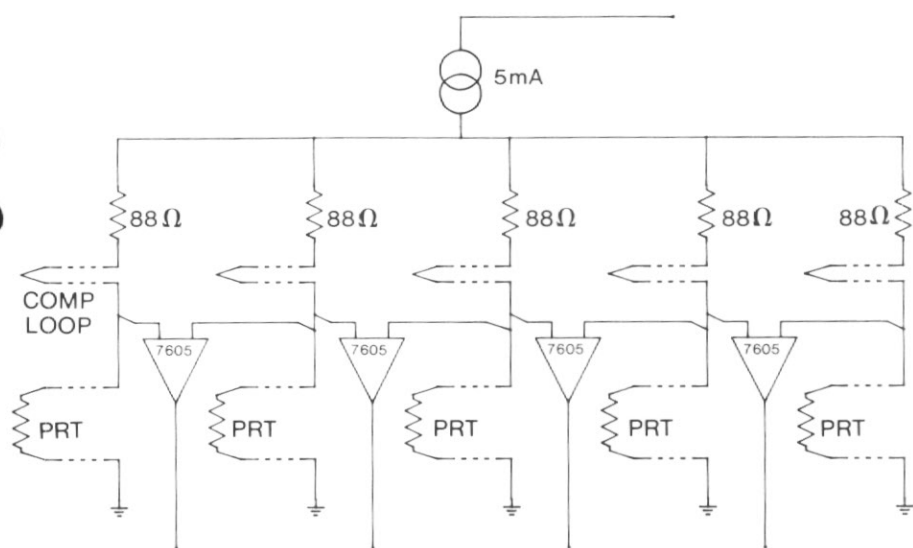


Fig. 5. Schematic diagram of the bridge used for temperature-difference measurements. PRT, platinum-resistance thermometer. Comp. loop, compensation loop.

can be reflected into the shielding through the lower aspiration port. This reflection of incident radiation could introduce scatter, if not a systematic offset into the measurements. Data collected during the zeroing calibrations at the beginning of the experiment suggest that radiation sensitivity at Halley during summer could be as high as  $1 \times 10^{-3} \text{ K (W m}^{-2}\text{)}^{-1}$ . Rough calculations show that typical values of reflected radiation entering the bottom aspiration vent could heat the airflow by  $0.03 \pm 0.01 \text{ K}$ , although if this radiation impinged upon the PRT directly, the apparent heating would be greater. Most of the STABLE measurements were made during the dark months of winter, so solar radiation errors were not a problem.

The AC aspirators gave a stated airflow of  $4 \text{ m s}^{-1}$  past the PRTs. This was reduced at times of heavy riming due to the lower vent becoming blocked. Occasionally, rime build-up would stop the fan, but this could be cleared by gentle probing with fingers. The lowest aspirator failed towards the end of the winter with jammed bearings. Rime always affected the lowest instruments most, and it is thought that this could have been part of the cause. The aspirator started working again of its own accord once the incoming solar radiation increased, although temperatures were still below  $-15^\circ\text{C}$ .

The temperature-difference values were obtained from a difference bridge (Fig. 5) directly, as opposed to finding the individual temperatures of the PRTs. The bridge used a constant current device to feed  $5.0 \text{ mA}$  into the five legs, thus giving about  $1 \text{ mA}$  through each PRT. This ensured immeasurable self-heating. Balance resistances of  $88 \Omega$  were used to ensure maximum linearity at around  $-30^\circ\text{C}$ , the expected operating temperature of the sensors. Bridge outputs were amplified by buffered 7605 commutating auto-zero operational amplifiers operating at a gain of 800. The bridge design was based on circuits supplied by the Boundary Layer Branch of the Meteorological Office.

The compensation loop arrangement shown in Fig. 5 will only provide perfect compensation for lead resistance changes if all connection leads and compensation loops have the same resistance. Unfortunately the leads from the base of the mast to the sensors were not of equal length, so the 'zero' reading from the bridge (all PRTs of the same resistance) was a function of the PRT and lead resistances, hence of ambient temperature. We have estimated the variation in zero offset with ambient temperature from the data gathered during the experiment by assuming that the lowest bridge reading obtained at a given temperature corresponded to neutral stratification, hence no temperature difference between the PRTs. These bridge readings were then taken as zero offsets. A simulation of the bridge equations using a 'spreadsheet' model which incorporated the variation of lead and PRT resistance with temperature, gave a very similar functional dependence. This model was also used to obtain calibration functions for the bridge over a wide temperature range, since the bridge response is only linear if the PRT resistance is nearly equal to that of the balancing resistor. In our analysis of the data, we have used a calibration equation of the form

$$\Delta T = a(1 - bT)(V - (V_0 + cT)),$$

where  $\Delta T$  is the temperature difference between sensors,  $T$  is the ambient temperature,  $V$  is the amplified bridge output voltage,  $V_0$  is the offset voltage at  $T = 0^\circ\text{C}$  and  $\Delta T = 0 \text{ K}$ ,  $a$  is the overall calibration factor,  $b$  is the coefficient of change of gain and  $c$  is the coefficient of change of offset.

Zero offset voltages,  $V_0$ , of the whole system (sensors/bridge/amplifiers) were found by running all sensors at the same level at the beginning and end of the experiment. Temperature coefficients of the PRTs were assumed from the standards and, together with the bridge equations and measured amplifier gain, were used to

calculate the overall calibration factors,  $a$ . Using 12-bit digitization gave a resolution of 0.0015 K and we estimate that the accuracy of the temperature differences was about 0.05 K. The bridge amplifier zeros and gains were checked weekly. No significant drift of either occurred during the experiment.

### *Sodar*

The Sodar operated at a frequency of 2300 Hz and a power of 120 W. Pulse lengths of 30 or 120 ms could be selected and the pulse rate was approximately one every 9 s. Echoes were displayed as a time-height record on a facsimile recorder. The chart width was 200 mm and the chart speed 30 mm per hour. Two stylus sweep speeds were available, making the chart width represent either 500 or 1000 m vertical range. The recorder gain could be adjusted to suit ambient noise levels.

The acoustic antenna comprised a 1.3-m diameter parabolic dish with a loudspeaker at its focus surrounded by a 2-m high acoustic enclosure. It was mounted vertically on a platform initially about 1 m above the surface. The dish was fitted with 800-W heating elements which proved sufficient to remove any rime which formed or any drift snow which entered the enclosure. It was not found necessary to cover the antenna during periods of falling or drifting snow.

Background noise at the site was generally low and the system could be operated at high gain under light wind conditions. However, surface winds of greater than  $8 \text{ m s}^{-1}$  generated sufficient noise in the antenna to render the system inoperable. The shorter pulse length was usually selected to maximize resolution. Echoes from above 500 m were rarely observed so the facsimile recorder was usually set to display this shorter range. Weak fixed echoes were observed on the chart during strong surface inversion conditions. They appeared to be caused by the various huts marked on Fig. 2.

### *Energy-balance instruments*

The heat balance over a typical snow surface was measured using a net flux radiometer and a vertical array of temperature sensors buried in the snow, extending to an initial depth of 1 m. A Kew-pattern radiation balance meter, calibrated by the Meteorological Office, was used to measure the net radiative flux over a relatively undisturbed area of snow that was thought to be typical of snow cover around Halley. We picked an area east of the logging hut to ensure that the prevailing easterly winds did not cause a wind tail to form over the site. The instrument was deployed with the flux plate pointing north to minimize shadow effects during the summer. Output from the flux plate was fed directly into a 7605 buffered commutating auto-zero operational amplifier operating at a gain of about 900. The instrument was occasionally affected by blown snow entering the aspirator port and blocking the fan. Not only did the reduced or stopped flow alter the sensitivity of the instrument but frost could then build up on the flux plate, altering the reflectivity of its surface. The aspirator was brought indoors and thawed whenever this happened. It is thought that pointing the radiometer so that the aspirator port faces west (a rotation of  $180^\circ$ ) would prevent this. Since shadow errors are not important during the dark winter months, this would have had little effect on the majority of the measurements.

Buried near the radiometer were five miniature platinum-resistance thermometers (Thermal Developments Inc. P100, to B.S. 1904) at initial depths of 0.05, 0.10, 0.25, 0.50 and 1.00 m, with the 0.25-m probe being a duplex sensor. The PRTs were encased in ceramic cylindrical probes of 2-mm diameter and 10 mm long with their axes

horizontal to minimize disturbance. All but the deepest probe were mounted on a thin wooden spar which allowed them to be raised as snow accumulated over the site, thus maintaining their original depths. The deepest probe was allowed to bury deeper during the year, with regular depth readings being taken from a graduated pole.

The PRTs were connected to a difference bridge identical to that used by the air temperature sensors (see p. 73). The cabling to the probes was run just under the surface to avoid altering the site albedo to a measurable degree. The absolute snow temperature was measured at 0.25 m using the second half of the duplex PRT at that level. This PRT was connected to a normal resistance bridge. Outputs from the difference bridge and resistance bridge were amplified by buffered 7605 commutating auto-zero operational amplifiers operating at a gain of about 800.

The snow temperature profile, due to its simplicity and lack of moving parts, functioned throughout the experiment. Accumulation always occurred during blizzard conditions, with the snow being deposited during the first half of the blizzard. The latter stages, especially when the wind speed was falling, would see removal of drift snow reducing the accumulation again. Raising the probe and cabling would have to be left until it was thought that no more drift ablation would occur, otherwise the probe could be left too high and it was impossible to push the probe back into the back-filled hole. Leaving raising for too long after accumulation had ceased would allow the powder to form into normal packed snow surface, and cable raising would leave a ragged surface.

Zero offset voltages of the whole system (sensors/bridge/amplifiers) were found by burying all the PRTs next to each other to a depth of 0.10 m at the beginning of the experiment before they were attached to the spar. Amplifier zeros and gains were checked weekly as for the air-temperature-difference bridge. No significant drift of either occurred during the experiment.

#### CONCLUSIONS

It has been demonstrated that modern robust micrometeorological instrumentation is well able to withstand the rigours of an Antarctic winter. The very low temperatures experienced cause few direct problems, but icing conditions and blowing snow may affect instrument performance. Cup-anemometers are particularly affected by icing.

Halley offers an ideal site for studying the stable boundary layer. Much insight has already been gained from STABLE and further data analysis is still required. It is hoped that related experiments may be conducted in this 'natural laboratory' in future years.

#### ACKNOWLEDGEMENTS

D. W. S. Limbert carried out the early planning for STABLE and gave us assistance and encouragement throughout. We are grateful to staff of the Meteorological Office Boundary Layer Branch, particularly P. J. Mason, B. A. Callander and D. M. Moore, for advice on instrumentation. Many members of the British Antarctic Survey contributed to the success of the project and we would especially like to thank R. I. Kressman, M. Pinnock and J. T. E. Turton. Finally we must thank the 1986 Halley wintering team for supporting P.S.A. during the field phase of the project.

*Received 2 October 1987; accepted 15 November 1987*

## REFERENCES

- ADACHI, T. 1974. Characteristics of wind and temperature fluctuations above the sloping surface at Syowa Station, Antarctica. *Journal of the Meteorological Society of Japan*, **52**, 82-5.
- BUSINGER, J. A., WYNGAARD, J. C., IZUMI, Y. and BRADLEY, E. F. 1971. Flux-profile relationships in the atmospheric surface layer. *Journal of Atmospheric Sciences*, **28**, 181-9.
- CAUGHEY, S. J., WYNGAARD, J. C. and KAIMAL, J. C. 1979. Turbulence in the evolving stable boundary layer. *Journal of Atmospheric Sciences*, **36**, 1041-52.
- DARBY, M. S. and MOBBS, S. D. 1987. Observations of internal gravity waves in the stably-stratified atmospheric boundary layer. (In PUTTOCK, J. S. ed. *Proceedings of the IMA Conference on Stably Stratified Flow and Dense Gas Dispersion*. Oxford University Press.)
- KAIMAL, J. C. 1969. Measurement of momentum and heat flux variations in the surface boundary layer. *Radio Science*, **4**, 1147-53.
- KING, J. C., MOBBS, S. D., DARBY, M. S. and REES, J. M. 1987. Observations of an internal gravity wave in the lower troposphere at Halley, Antarctica. *Boundary-Layer Meteorology*, **39**, 1-13.
- OBAYASHI, S. and ISHIDA, T. 1979. Some characteristics of turbulence in katabatic winds over Mizuho Plateau, East Antarctica. *Antarctic Record*, **67**, 75-85.
- KÖNIG, G. 1985. Roughness length of an Antarctic Ice Shelf. *Polarforschung*, **55**, 27-32.
- MBERT, D. W. S. 1963. The snow accumulation at Halley Bay in 1959, and associated meteorological factors. *British Antarctic Survey Bulletin*, No. 2, 73-92.
- REES, J. M. and MOBBS, D. S. 1987. Studies of internal gravity waves at Halley base, Antarctica, using wind observations from three masts. Submitted to *Quarterly Journal of the Royal Meteorological Society*.
- THOMAS, R. H. 1973. The dynamics of the Brunt Ice Shelf, Coats Land, Antarctica. *British Antarctic Survey Scientific Report*, No. 79, 49 pp.
- TRIBBLE, D. T. 1964. Snow surface studies. (In BRUNT, D. ed. *The Royal Society International Geophysical Year Antarctic Expedition. Halley Bay, Coats Land, Falkland Islands Dependencies, 1955-59*, vol. IV. London, Royal Society.)
- WEBB, E. K. 1970. Profile relationships: the log-linear range and extension to strong stability. *Quarterly Journal of the Royal Meteorological Society*, **96**, 67-90.